Classical Path Analysis of End-Grafted Dendrimers: Dendrimer Forest

Galen T. Pickett

Department of Physics and Astronomy, California State University, Long Beach, 1250 Bellflower Blvd., Long Beach, California 90840

Received May 29, 2001; Revised Manuscript Received August 20, 2001

ABSTRACT: I consider a brush consisting of dendritic polymer end-grafted by its initial segment to a flat, impenetrable surface, in both the molten and solvated cases. The parabolic profile of linear grafted brushes is maintained, but the distribution of the free tips is quite different from the linear brush case. In particular, free ends are comparatively buried in the brush or "forest" layer compared to linear chains, an effect which is magnified by going to higher and higher generations. There is no appreciable tendency for dendritic arms to fold backward into the layer, however. The results of the classical path analysis compare favorably to lattice self-consistent-field calculations on the same systems.

1. Introduction

Dendrimers are branched macromolecules, with a topology similar to a Caley lattice or tree structure.[1] There is great synthetic freedom in the design of these molecules,[2−5] so that the dendrimer can consist of a combination of hydrophobic and hydrophilic chain segments and whose tips can be decorated with arbitrary functionality. Thus, the self-organization of single dendrimer molecules is of considerable interest for a range of practical applications spanning controlling microdomain morphology[6,7] to creating templates for nanometallic clusters.[8] Indeed, the most important technological issues for homogeneous dendrimers (all branches and tips have the same composition) are the equilibrium distribution of segments (is the dendrimer hollow[9] or is it filled[10−12]), and the location of terminal groups (exposed or buried) are only gradually being addressed experimentally,[13] although the theoretical picture is somewhat clearer.[10−12,14−16]

One role where many functionalized ends combined with a large density of passive segments is required is in the design of protective coatings with specific interactions.[17,18] Such end-grafted polymer "brushes" are useful in controlling colloidal interactions,[19−21] in describing the thermodynamics of block copolymer microsegregation,[22] and in providing a thermodynamic and mechanical control on liquid crystalline order.[23,24] As the free ends of polymer chains can be functionalized with biologically specific ligands, expanding the number and nature of these functionalized sites can be achieved by end-grafting polymers with more exotic architectures than linear homopolymers. For example, end-grafting many-armed star macromolecules has been suggested as an efficient means of preventing unspecific protein adsorption combined with specific adhesion of target molecules to make biologically "smart" surfaces.[25]

Dendrimer molecules could be thought to behave similarly to these end-grafted star layers. These dendrimer polymers combine high local concentration of monomers (good to provide an osmotic barrier for surface protection) with a geometric proliferation of funtionalizable free ends. As such, they could offer advantages for controlling surface properties through end grafting at the first "root" monomer of the treelike molecule, with a single strand proceeding as the "trunk", which regularly splits into chemically identical branches, forming a "forest" as in Figure 1A. A conventional polymer brush is thus a "G1" (first generation) forest of bare trunks. These linear brushes in good solvent, but at high grafting density, are characterized by a distribution of chain free ends strongly peaked away from the grafting surface (and hence are available for engineering applications), while the average polymer segment density is a maximum at the grafting surface and falls off parabolically with distance away from the grafting surface, z: $\phi(z) \sim (1 - z^2/h^2)$, where h is the overall height of the grafted layer.[18] It should be noted that *annealed* random branching of such a forest has been considered in a self-consistent-field calculation, where the degree and location of branching are adjusted to be in thermodynamic equilibrium.[26] Such annealed forests are virtually identical to linear polymer brushes. (Indeed, they act as brushes of effective linear polymers, and the branchings are systematically exported to the free surface!) What I consider here is not quite the same thing. The branchings are not disordered, but they are quenched and therefore locked in permanently during the calculation. The difference between such a quenched and an annealed chain architecture is dramatic, as I show below. As the annealed architecture is particularly hard to conceive of in a real synthetic chemistry context, it is hard to think of those annealed results as having physical significance.[27]

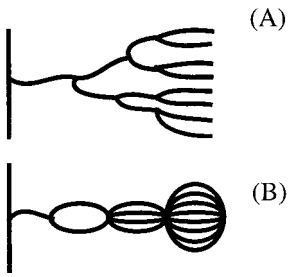

Figure 1. Schematic: (A) Dendrimer forest, here with G4 molecules. A priori, the arms of each dendrimer are free to take independent conformations. A typical dendrimer is shown in bold. (B) In the classical limit, all of the chain ends on a single dendrimer occur at the same height above the "floor" of the forest. Likewise, each of the subbranches span the *same* distances. (C) Equivalent molecule considered in the classical path approximation. All monomers of equivalent chemical rank are held at the same distance from the grafting surface.

10.1021/ma010917y CCC: $20.00
Published on Web 11/06/2001

In this paper, I consider the static properties of an end-grafted brush of G2−G5 dendrimer under both good solvent (although concentrated) and poor solvent conditions. Adding branches to the macromolecule enhances dramatically the effect of the steric interactions which cause the chains to stretch away from the surface. Thus, dendritic polymers can be expected to behave in almost all respects as being "more perturbed" from ideal statistics than their linear topology analogues. With this insight, it is clear that the so-called "classical path" analysis of the brush[18] should generally be an even *better* description for the dendrimer forest. The classical path ansatz is essentially a saddle-point approximation to the single-chain free energy in a self-consistent manner. The classical path analysis for the dendrimer brush maintains the one important feature of the linear polymer brush: a parabolic segment density for concentrated, although not molten, forests. The distribution of chain tips is distorted, however, forcing a great many of the extra tips into the forest where they may not find much useful employment. The results of the classical path self-consistent approach are checked against lattice self-consistent-field calculations and are found to compare quite well.

2. SCF Classical Path

Let σ dendrimers per unit area be grafted to a flat, impenetrable surface located at $z = 0$ as in Figure 1. Each of these G-generation molecules has 2^{G-1} free ends (G4 in Figure 1) and N monomers in each of its $2^G - 1$ subarms. Consider a linear subsegment of this dendrimer, taking up n_0 monomers and proceeding from $z = z_0$ to $z = z_1$. The free energy of this chain segment is

$$S[z(n)] = \int_0^{n_0} \mathrm{d}n \left(\frac{1}{2a^2} \left| \frac{\mathrm{d}z}{\mathrm{d}n} \right|^2 + P(z(n)) \right) \tag{1}$$

where a is the size of a single monomer. This subsegment can be constructed by bringing dn monomers at at time to the height $z(n)$, each entailing a free energy cost $P(z)$. This segment can then be aligned so that its ends extend from z to $z + \mathrm{d}z$. Adding up all the costs for each dn-length subchain, the expression in eq 1 is obtained. At this point, the insertion potential, $P(z)$, is unknown but will be determined self-consistently later. The classical path approximation amounts to demanding that each of the $0...n_0$ monomers are located so that $S[z(n)]$ is minimized. This is accomplished when

$$\frac{1}{a^2} \frac{\mathrm{d}^2 z}{\mathrm{d}n^2} - \frac{\mathrm{d}P}{\mathrm{d}z} = 0 \tag{2}$$

Thus, given the initial extension of the chain segment, $\mathrm{d}z/\mathrm{d}n|_{z=z_0}$, the location of *every other monomer* in the chain segment is uniquely determined. As this must be true for every chain segment on a given dendrimer in the forest, it must be that all 2^{G-1} ends of a given dendrimer are at the *same* height above the grafting surface. Indeed, each monomer on the dendrimer can be labeled by the chemical index, n, equal to the number of monomers along a direct line of descent toward any of its daughter free tips. Thus, for all free-end monomers, $n = 0$, and the grafted monomer is located at $n = GN$, the first branching into two subchains occurs at $n = (G - 1)N$ and so on (Figure 1C). The first conclusion of the classical analysis is that, on a single dendrimer, all monomers with the same chemical index n are located at the same height above the grafting surface.

Calculating the free energy of an entire dendrimer is now possible through defining the branching number, $f(n)$, equal to the number of equivalent chain segments at a particular index, n. Thus

$$\begin{aligned} f(n) &= 2^{G-1} \quad \text{when } 0 < n < N \\ f(n) &= 2^{G-2} \quad \text{when } N < n < 2N \\ &\vdots \\ f(n) &= 1 \quad \text{when } (G-1)N < n < GN \end{aligned} \tag{3}$$

With these conventions, the free energy of the entire dendrimer, whose free ends are held at the location z_0, is

$$S_{\mathrm{tot}}[z(n)] = \int_0^{GN} \mathrm{d}n\, f(n) \left[\frac{1}{2a^2} \left| \frac{\mathrm{d}z}{\mathrm{d}n} \right|^2 + P(z(n)) \right] \tag{4}$$

the integral being evaluated subject to the constraint that $z(0) = z_0$ and $z(GN) = 0$ and further that the chain extension at the free end vanishes: $\mathrm{d}z/\mathrm{d}n|_{z=z_0} = 0$. Minimizing S_{tot} under these conditions amounts to determining the classical motion of a particle with a *time-dependent mass* $f(n)/a^2$. Thus, the particle initially has a mass of $2^{G-1}/a^2$, it gets cut in half when time exceedes N, it gets cut in half again when the time exceeds $2N$, etc., proceeding in this way until the particle has a mass of $1/a^2$ during the last leg of its motion. The potential this particle responds to, $-f(n)P(z)$, is also time-dependent, but in a separable way. Furthermore, this classical particle is released from rest, and regardless of the "height" from which it is dropped, it always arrives at $z = 0$ in the same amount of "time" $= GN$. As long as free ends of the dendrimer molecule exist throughout the forest (i.e., there are no end-free or "dead" zones), the unique potential with vanishing $P(z=h)$ that makes this possible is the harmonic oscillator potential,

$$P(z) = \frac{1}{2} \frac{\omega^2}{N^2} (h^2 - z^2) \tag{5}$$

where h is the overall layer height as in the brush case. Thus, the "equal-time" potential of the linear, G1 polymer brush survives the (regular, quenched) branching of the chain. The dimensionless frequency of the parabolic potential ω is, as yet, unknown but can be determined by examining the trajectory of this classical particle, $z(z_0,n)$.

With the time-independent portion of the potential given by eq 5 the trajectory must be broken into several piecewise-smooth portions, each of the form

$$z_g(z_0,n) = A_g \cos \omega \frac{n}{N} + B_g \sin \omega \frac{n}{N} \tag{6}$$

where $z_1(z_0,n)$ is the trajectory of the particle during $0 < n < N$ and $z_G(z_0,n)$ is the trajectory of the particle during $(G - 1)N < n < GN$. The initial conditions on the trajectory are that $z(z_0,0) = z_0$ (the particle starts at the initial height z_0) and that $(\mathrm{d}z/\mathrm{d}n)|_{n=0} = 0$ so that

$$A_1 = z_0 \quad \text{and} \quad B_1 = 0 \tag{7}$$

Table 1. Classical Path Dimensionless Frequency ω_G

G	$\cos^2 \omega_G$	$\omega_G NG$
1	0	1.570 796 326
2	$^2/_3$	1.230 959 417
3	$^8/_9$	1.019 510 728
4	$^1/_9(5 + \sqrt{13})$	0.843 642 816
5	$^2/_3(1 + \sqrt{2}/3)$	0.692 568 421

Continuity of the trajectory requires that

$$z_g(z_0,gN) = z_{g+1}(z_0,gN) \quad \text{for } g = 1, ..., g = G \tag{8}$$

Equivalently

$$A_g \cos \omega g + B_g \sin \omega g = A_{g+1} \cos \omega g + B_{g+1} \sin \omega g \tag{9}$$

Mechanical stability (or, equivalently, the minimization of the free energy, eq 4) requires that the *momentum* of the particles be continuous at $n = N$, ..., $n = GN$, which requires that the chain *velocity* $\equiv$ (dz/dn) be *discontinuous*:

$$f(0) \frac{\mathrm{d}z_1}{\mathrm{d}n}|_{n=N} = f(N) \frac{\mathrm{d}z_2}{\mathrm{d}n}|_{n=N} \tag{10}$$

As there are *twice as many chain segments* with $n = N^-$ as there are with $n = N^+$, those chains with $n = N^+$ must be stretched out twice as much in order to maintain mechanical equilibrium. Thus

$$\frac{\mathrm{d}z_{(g+1)}}{\mathrm{d}n}|_{n=gN} = 2 \frac{\mathrm{d}z_g}{\mathrm{d}n}|_{n=gN} \tag{11}$$

or equivalently

$$2 = \frac{-A_{g+1}\sin \omega g + B_{g+1}\cos \omega g}{-A_g \sin \omega g + B_g \cos \omega g} \tag{12}$$

The system of equations, eqs 7, 9, and 11, uniquely determines all of the A_g and B_g. The unknown frequency parameter, ω, can then be determined by requiring that

$$z_G(z_0,GN) = 0 \tag{13}$$

In general, eq 13 is a polymonial of degree $G - 1$ in cos(ω). Of the many solutions to this polynomial, there is a unique choice that satisfies $z(z_0,n) > 0$ for all $0 < n < GN$. Table 1 shows the values of ω required for each of $G = 1...5$, and Figure 2 shows the trajectories as determined this way.

Thus, quite generally, the insertion potential per monomer is known and has the same functional form under a broad set of circumstances. Given that the potential is fixed by the "equal time" constraint, the requirement the potential be self-consistently generated from the chain statistics seems to be fulfilled but is not in fact so. The parabolic form for $P(z)$ in eq 5 depends on the assumption that free ends are located throughout the brush. Thus, to close the problem, we need to specify how many dendrimer chains terminate at each height z of the brush. Once that has been calculated, and verified to be nonzero, self-consistency and the classical limit of the problem are achieved.

Let $\xi(z)f(0)$ be the density of free ends located at the height z. Note that the multiplicity of ends is accounted for by the factor $f(0) = 2^{G-1}$. The volume fraction of monomers in the brush at the height z, $\phi(z)$, is

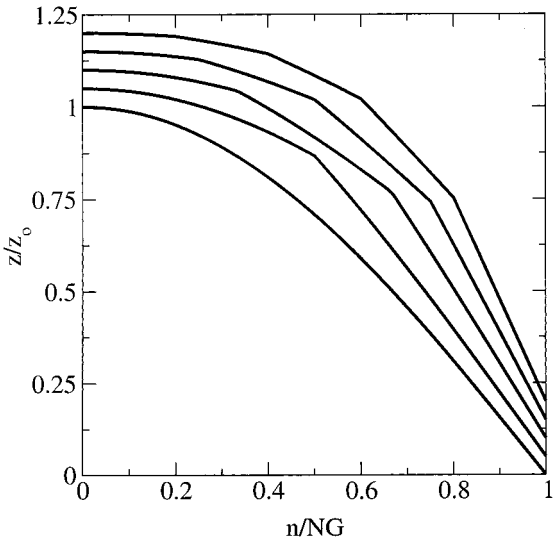

Figure 2. Classical path trajectories. Shown are scaled trajectories, $z(z_0,n/GN)/z_0$, for $G = 1...5$. The trajectory for $G = 1$ is clearly harmonic, and for all $G \neq 1$, the trajectories are piecewise harmonic. The trajectories for $G = 1$, ..., $G = 5$ are shown offset in the y direction by $0.05G$ for clarity.

$$\phi(z) = \int_z^h \mathrm{d}z_0 \, \phi(z;z_0) \, \xi(z_0) \tag{14}$$

where $\phi(z;z_0)$ is the volume fraction taken up at the height z by all of the monomers on a chain whose free end is located at the height z_0. As in the analysis of ref 18,

$$\phi(z;z_0) = \frac{1}{\mathrm{d}z/\mathrm{d}v} f(n(z;z_0)) \tag{15}$$

Self-consistency is then guaranteed by adjusting $\xi(z) > 0$ so that either of two conditions is met. First, if the brush is a dry, molten brush, it is appropriate to require that

$$\phi(z) = \text{const} \tag{16}$$

In this case, the overall height of the brush is given by the relation that the brush is entirely taken up with monomers from the dendrimers:

$$\frac{h}{\sigma} = N(2^G - 1)a^3 \tag{17}$$

On the other hand, if the brush is effused with solvent, then the cost to insert a monomer at the height z is given from a virial expansion as proportional to the fraction of sites already taken up by the monomers. In other words, $\xi(z)$ should be tuned so that

$$w\phi(z) = P(z) = {}^1/_2 \frac{\omega^2}{N^2}(h^2 - z^2) \tag{18}$$

Here, w is the second virial coefficient of the monomer−monomer interaction. Thus, we should adjust $\xi(z)$ so that the *monomer density* is parabolic. In this case, it is a simple matter to determine the height, h of the brush from the constraint that

$$\int_0^h \mathrm{d}z \, \phi(z) = \sigma N(2^G - 1) \tag{19}$$

giving

$$h = aN(3w\sigma(2^G - 1)/\omega_G^2)^{1/3} \tag{20}$$

Note that in both cases $h \approx N$. We shall check these expressions below numerically.

3. Scheutjens and Fleer Lattice SCF

To explicitly check the predictions of the classical path analysis, I execute calculations with the lattice self-consistent-field method of Scheutjens and Fleer.[19] The architecture of the dendrimer chain is fixed during the calculation (i.e., the chain architecture is *quenched* and completely without disorder). The arms of the dendrimer are fixed at N monomers, and there are G generations in the chain. There is but a single type of monomer in these calculations, both in the melt state and in the solvent-swollen case. Thus, the dendrimer brush is in contact with some amount of its (athermal) monomeric solvent.

Given, $P(z)$, here as in the classical path analysis, the free energy cost per monomer to insert a monomer at the position z in the lattice, the statistics of a single dendrimer can be determined. First, we define the Boltzmann weight associated with P:

$$g(z) = \exp[-P(z)] \tag{21}$$

where the energy scale is explicitly taken to be the thermal scale, $kT \equiv 1$. Let $\mathcal{G}_1(z)$ be the total statistical weight associated with a linear chain of length N with one end located at z, in the given potential field $P(z)$. This weight can be built up through the recursion relation:

$$G(z,z';1,1) = g(z)\delta_{z,z'}$$
$$G(z,z';1,n) = \langle G(z,z';1,n-1)\rangle g(z)$$
$$\mathcal{G}_1(z) = \sum_{z'} G(z,z';1,N), \tag{22}$$

where $G(z,z';1,n)$ is the statistical "propagator", or unnormalized statistical weight, of a linear chain segment proceeding from z to z' expending n monomers. Here, the angled brackets indicate a sum over nearest-neighbor lattice sites:

$$\langle g(z)\rangle = \lambda_1 g(z-1) + \lambda_0 g(z) + \lambda_1 g(z+1) \tag{23}$$

for example, where $\lambda_1 = {}^1/_6$ and $\lambda_0 = {}^2/_3$ accounts for the fraction of nearest neighbor sites (on a simple cubic lattice with a total of six nearest neighbors). With the statistical weight $\mathcal{G}_1(z)$, the full statistical weight attributed to the dendrimer can be determined. I define

$$\mathcal{G}_M(z) = \sum_{z'} G(z,z';1,N)\langle \mathcal{G}_{M-1}(z')\rangle \tag{24}$$

That is, $\mathcal{G}_2(z)$ is the total weight associated with a strand of N monomers beginning at z, proceeding to any z' where it is met by two strands of length N. Clearly, the entire weight of the dendrimer is given by

$$\text{weight} = \mathcal{G}_G(1) \tag{25}$$

Figure 3 shows diagrammatically this interpretation for the case of G4.

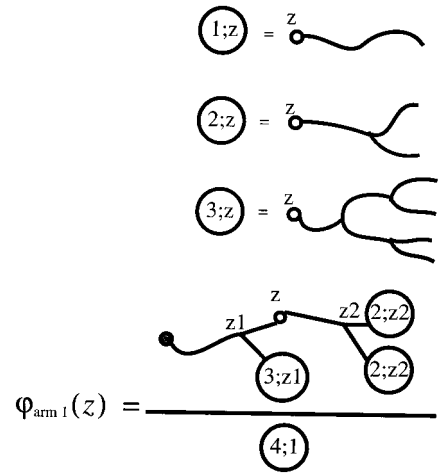

Figure 3. Architecture of the dendrimer in the lattice SCF model. Here, I show schematically (top to bottom) $\mathcal{G}_1(Z) - \mathcal{G}_3(z)$ as well as a term in the calculation of $\phi(z)$ corresponding to the sth monomer of the first major branch of the grafted dendrimer.

Given $\mathcal{G}_M(z)$, all relevant statistical averages can be made. In particular, the volume fraction due to the sth monomer on one of the two of the principle branches of the dendrimer can be calculated as

$$\phi_s(z) = \sigma \sum_{z_1,z_2} \times \frac{G(1,z_1;1,N)\langle \mathcal{G}_{G-1}(z_1)\rangle G(z_1,z;1,s)G(z,z_2;s,N)\langle \mathcal{G}_{G-2}(z_2)\rangle^2}{\mathcal{G}_G(1)g(z)} \tag{26}$$

where the additional factor of $g(z)$ in the denominator cancels out the double weighting of the s monomer taken by the two factors of G. The initial factor of σ ensures that, for every $1/\sigma$ of grafting surface area, there is found exactly one such monomer. This formula is shown somewhat more transparently in Figure 3. Thus, given $P(z)$, all of the statistics of the grafted brush can be calculated. In particular,

$$\phi_{\text{tot}}(z) = \phi(z) + \phi_{\text{solvent}}(z) \tag{27}$$

can be calculated. Self-consistency is enforced on $P(z)$ when $\phi_{\text{tot}}(z) = 1$; that is, each lattice site is completely filled by a combination of solvent monomers and monomers attached to a grafted dendrimer. The incompressibility constraint represents L highly nonlinear equations in the L unknown values of $P(z)$, where L is the total size of the lattice. The required values of $P(z)$ are determined through standard numerical methods.[19,28] I note that this requirement is not in general satisfied in an earlier SCF treatment of single dendrimers[12] although the qualitative understanding of the single dendrimer arrived at there is correct.[29]

4. Results

Figure 4 shows the distribution of dendrimer free ends in the melt brush for G2−G5, as determined from the classical path approximation and from the lattice SCF calculations. In each case, the solid line represents a numerical solution to eq 14 based on the classical path approximation, and thus is *not* tied to the lattice approximations associated with Scheutjens and Fleer's

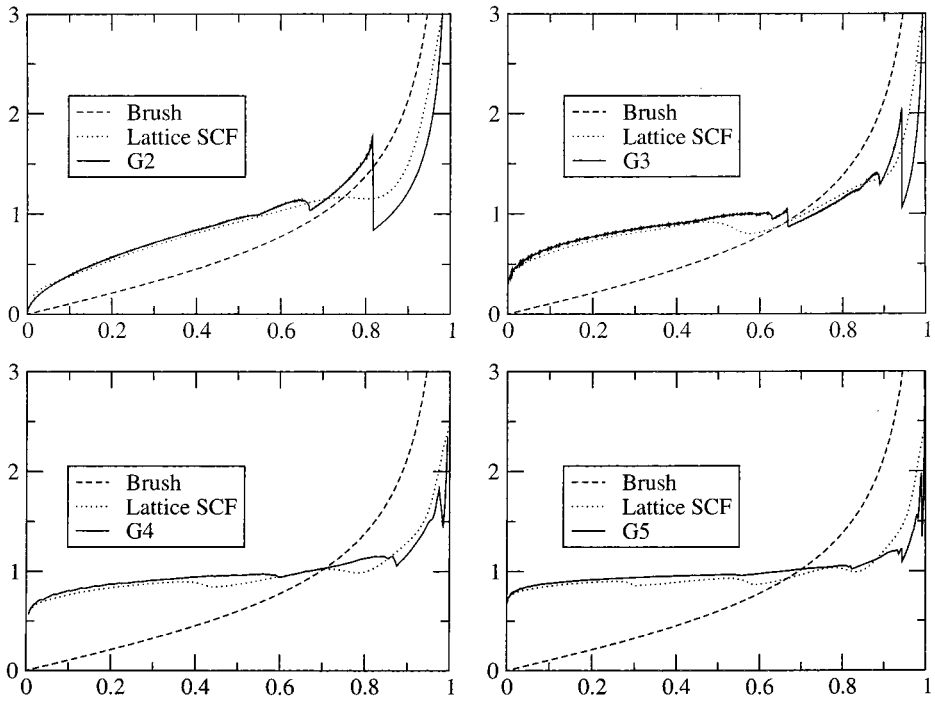

Figure 4. Melt forest end distribution. (A) G2. The solid line is the result of the classical path approximation, and there is a clearly visible discontinuity in the distribution of free ends at $z \approx 0.7h$. The dotted line is the result of a lattice SCF calculation with $N = 200$, $\sigma = 0.23$, and $h = 140$. The end distribution of a linear brush is shown as the dashed line for reference. (B) G3. Symbols and curves are as in (A). The lattice calculation was carried out with $N = 40$, $h = 70$, and $\sigma = 0.2425$. (C) G4. Symbols and curves as above. Here, $N = 30$, $h = 70$, and $\sigma = 0.14$. (D) G5 Here $N = 20$, $h = 70$, and $\sigma = 0.1$.

method, with parameters as listed in the figure caption. The dashed line shows the analytic distribution of free ends in a melt brush of linear chains, which vanishes near the grafting surface and diverges as $(h^2 - z^2)^{-1/2}$ near the top of the canopy of the forest. The dotted line shows the results of the numerical lattice calculations on the dendrimer of the appropriate generation. The "classical path" distribution of ends is only defensible, recall, if it is nonzero throughout the entire brush. The numerical results clearly bear this out.

The remarkably jagged distribution of free ends is easy to understand. The molten layer can be built up chain by chain (as is proposed in ref 18 quite generally) as follows. Consider first the G1 brush. The necessary concentration of free ends can be constructed by building up the brush chain by chain, distributing chain free ends from the top of the brush toward the grafting surface. Free ends are added to the top of the layer, one by one, until the upper surface at $z = h$ is completely filled with monomers. Proceeding into the brush, ends can be added at each height so as to completely fill up the remaining volume not taken up by monomers from chains with free ends already distributed higher up. The number of ends required to do this is alway nonnegative, as $\phi(z;z_0)$ is monotonic, increasing from $z = 0$ up to the location of the free end at z_0.

Now consider the G2 forest. Once the upper layer has been completely filled, the volume fraction taken up in the layer changes discontinuously at $z \approx 0.7h$, when the two free arms of the dendrimer merge into a single trunk strand. Now, continuing into the brush, I distribute free ends in the region $0.7h < z < h$. The discontinuity of occupied volume persists. The only way to make good this lost volume is to discontinuously add more and more free ends at $z \approx 0.7h$ until the unoccupied volume is completely filled up. Generally, for a generation-G forest, there will be $G - 1$ major discontinuities in $\xi(z)$ as is evident in Figure 4.

The results of the numerical SCF calculations shadow the classical path results nicely. In the classical path approximation, the height of the brush is the controlling length scale, so that the requirement that $\xi(z)$ be normalized controls its absolute value. This is so because for each chain-end location there is but a single chain trajectory that contributes to $\phi(z)$. In the SCF calculations, however, all paths are present, with the correct Boltzmann factors, so that fluctuations around the classical path smooth out the end distribution. The extent of the smoothing out is determined by the extent that these fluctuations occur. Thus, the first "kink" in the classical path end distribution is uniformly smoothed out. At the tip of the brush, fluctuations in the chain trajectories are most important as the chains are under vanishing tension as $z \rightarrow h$. Thus, random walk excursions from the classical path smear out the ideal placement of the ends. However, there is a characteristic inflection in the numerical end distribution located at this first kink. The rest of the major kinks in the free-end distributions are well matched by the lattice model, in both location and magnitude, although there is a considerable degree of smoothing in these ripples as well.

In Figure 5, I show the self-consistently determined insertion potential, $P(z)$, as determined in the numerical SCF calculations for the G2−G5 brushes. The solid line is the parabolic profile of the classical path analysis, and while there are systematic deviations from this prediction, it is not surprising as some of the assumptions regulating the interpretation of the lattice theory and the Gaussian form of the stretching energy in eq 4 are breaking down. In the G5 example, in particular, the height of the brush is $L = 70$, and the maximal

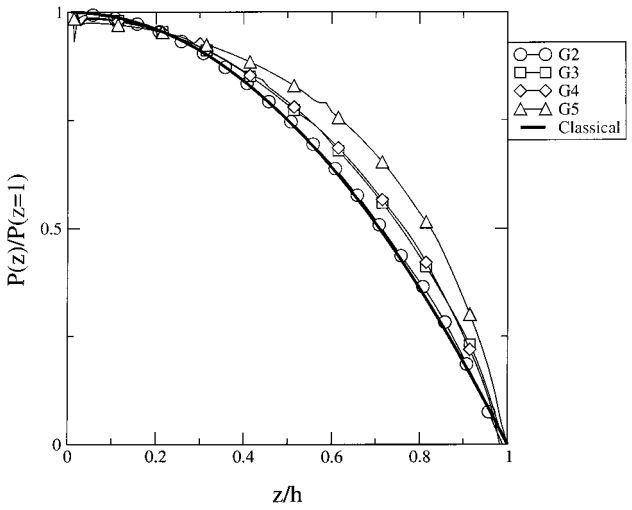

Figure 5. Melt brush potential profile. Insertion potentials, $P(z)$, for each of the cases in Figure 3 are displayed. They generally follow a parabolic format.

possible extent of the brush is $L_{max} = 5N = 100$. Thus, finite extensibility of the chains should play a role in determining $P(z)$ which is not taken into account in the classical path analysis. There is a broad agreement between the predictions of the classical path and the numerical analysis, however.

In Figure 6, I turn to the case of a less highly grafted brush, in the presence of a small molecule athermal solvent. Here, again, I show the end density as calculated in the classical path approximation (solid curve) and show a comparison to numerical lattice SCF calculations (dotted curve) and show the distribution of ends one expects in the classical limit of a linear brush (dashed line). Here, the classical end distribution is *continuous* although not smooth. Again, the classical path analysis and the lattice SCF approximations seem to confirm each other. As one passes from the linear brush to more and more generations in the dendrimer, free ends in the brush are progressively forced *toward the grafting surface* and away from the edge of the brush. However, as shown in Figure 7, the overall density of monomers is also highest at the grafting surface. The inset is the monomer density profiles scaled in magnitude as well as height. It is clear from the collapse of the data that the classical path prediction that $\phi(z)$ is parabolic is quite well verified.

5. Backfolding

There is the possibility that the correspondence between the classical path prediction and the lattice SCF calculations is a matter of accident. Free ends are definitely redistributed compared to the linear brush case by the data in Figures 4 and 6. Could it be that these ends are forced into the brush as the result of chains *folding back* on themselves in order to provide the necessary monomers to ensure self-consistency? Such backfolding conformations are strictly ruled out in the classical path calculations, as in Figure 1C. Backfolding conformations are in principle allowed in the numerical SCF calculations (Figure 1A), and the question is how much to they contribute to the overall properties of the grafted layer? Backfolding has been predicted to occur in G2 forests[7,30] as well as in layers of grafted stars.[25] They are also thought to be the key to understanding the generally accepted dense core picture of single dendrimer conformations.[10−13]

To make the inquiry concrete, I focus on the conditions of the G5 melt brush (lower-right entry of Figure 4). Clearly, the "trunk" chain segment (with chemical index $5N < n < 4N$) cannot "fold back" on itself because it is grafted to the impenetrable surface at $z = 0$. However, each subsequent branch can certainly do so. To evaluate this possibility, one can hold, for example, the branching point between the trunk segment and the first two major subbranches located at each of the lattice sites $1 < z < N$. With this junction held at a particular

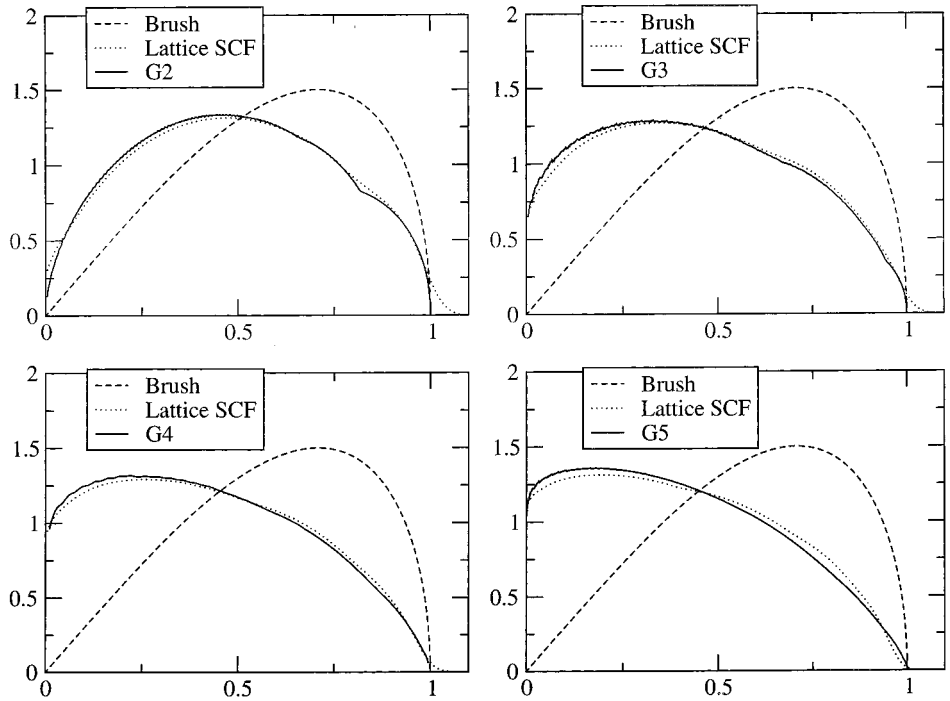

Figure 6. Solvated brush end distribution The curves in (A)−(D) have the same meaning as in Figure 3. Here, however, $N = 100$ for all of the forest layers, and $\sigma = 0.01$.

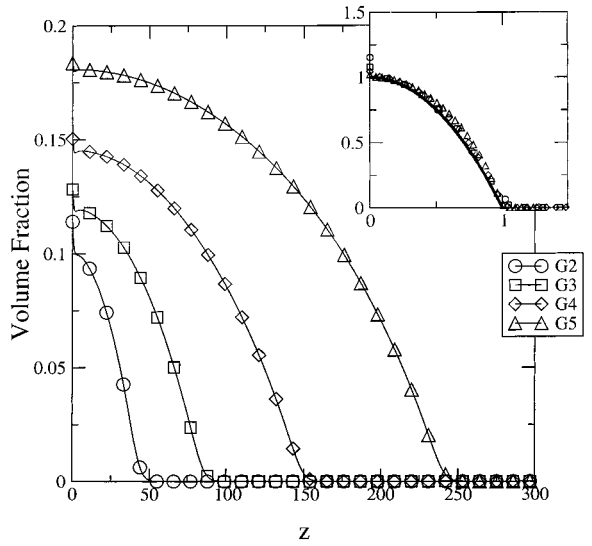

Figure 7. Solvated brush concentration profile. For the forest layers in Figure 5, I have plotted the volume fraction profiles of each of the G2−G5 layers. Inset: these profiles have been scaled with a comparison to the parabolic profile predicted by the classical path.

height, one can calculate the distribution function for the two ends of the first two subchains. If there is a significant amount of backfolding, then there will be an appreciable probability of finding the end-segment *closer* to the grafting surface than the initial segment. In the plots shown in Figure 8, this is done. The $n = 4N$ monomer is held at, for example, $z = 15$. Evidently, the other end of this subchain is nearly full stretched, located near $z = 30$. Backfolding on these sorts of plots would be indicated by having an appreciable density below the solid line. The extent of thermal fluctuations around the classical path can also be determined visually by the relative width of the end distribution—in this case very narrow. As can be seen, for *each* subchain, there is no appreciable backfolding. All statistically significant chain trajectories move *away* from the grafting surface as the chemical index is decreased. Thus, the presence of free ends near the grafting surface is evidence that there is a surprisingly large population of chains that are completely unstretched, with essentially all of their monomers executing very small deviations from $z = 0$. Instead of backfolding to bring their branches closer to the floor of the forest, a number of trees are *stunted in their growth* in order to build up the required density of monomers.

It has been suggested that just such backfolding occurs in the strongly stretched limit of linear/dendrimer block copolymers,[7] but in light of Figure 8 it is certain that this backfolding of the outer arms is a step toward approaching the parabolic potential distribution required in the end-distributed brush. Thus, it is possible that even in single molecule dendrimers such "backfolding" is responsible for the filling of the internal core. Certainly no backfolding occurs in the flat brush but could conceivably occur in brushes attached to curved substrates. The location of the onset of such backfolding would be an interesting problem for further analysis.

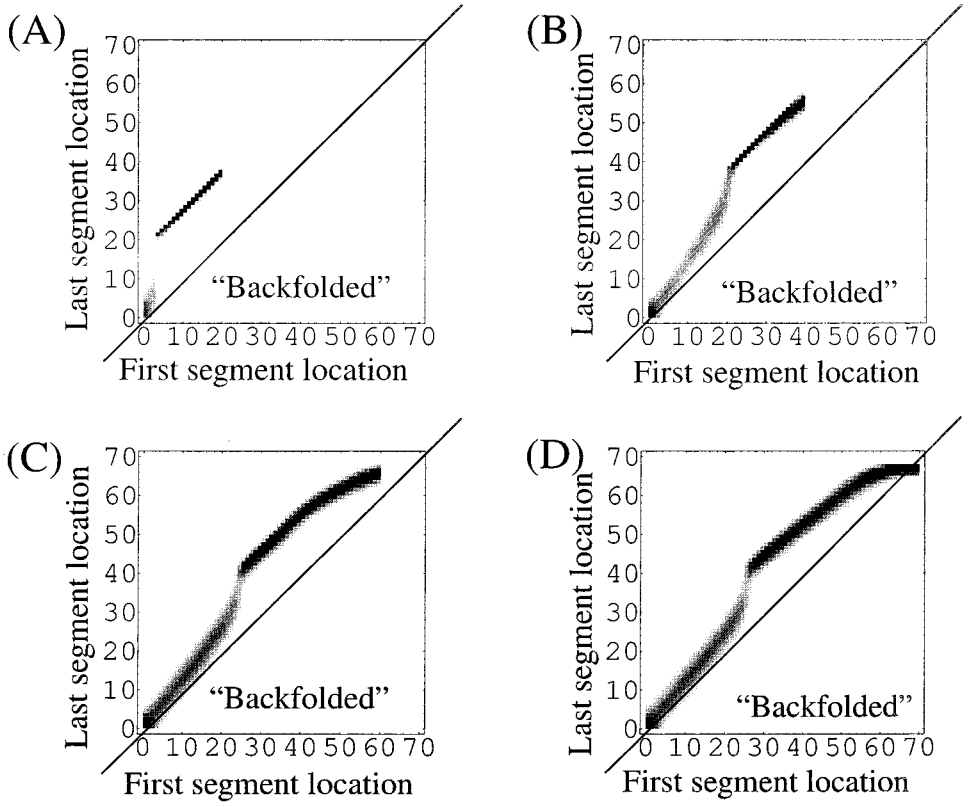

Figure 8. No backfolding for the dendrimer G5. (A) Holding the $n = 4N$ monomer at specific locations in the layer, the spatial distribution of the $n = 3N$ monomers is shown. The $3N$ monomers virtually always appear higher in the forest layer than the $4N$ monomers. (B) Similar plot as in (A) but looking at the distribution of the $2N$ monomers given the location of the $3N$ monomers. There is no sign of backfolding, which would appear as some weight for the $2N$ monomers to be found below the solid line. (C) and (D) show similar plots for the N and 0th monomers, respectively.

6. Conclusion

The dendrimer brush has been analyzed in the context of self-consistent-field theories in both the classical path and a numerical lattice model. These models agree in their details that the "parabolic" profile of the monomer insertion potential of linear grafted brushes is maintained, but the distribution of the free tips is quite different from the linear brush case. In particular, free ends are comparatively buried in the brush compared to linear chains, an effect which is magnified by going to higher and higher generations. There is no appreciable tendency for dendritic arms to fold backward into the brush, however.

References and Notes

(1) Voegtle, F.; Gestermann, S.; Hesse, R.; Schwierz, H.; Windisch, B. *Prog. Polym. Sci.* **2000**, *25*, 987.
(2) Ariga, K.; Urakawa, T.; Michiue, A.; Sasaki, Y.; Kikuchi, J.-I. *Langmuir* **2000**, *16*, 9147.
(3) Maraval, V.; Laurent, R.; Donnadieu, B.; Mauzac, M.; Caminade, A.-M.; Majoral, J.-P. *J. Am. Chem. Soc.* **2000**, *122*, 2499.
(4) Pan, Y.; Ford, W. T. *Macromolecules* **1999**, *32*, 5468.
(5) Watkins, D. M.; Sayed-Sweet, Y.; Klimash, J. W.; Turro, N. J.; Tomalia, D. A. *Langmuir* **1997**, *13*, 3136.
(6) Milner, S. T. *Macromolecules* **1994**, *27*, 2333.
(7) Frischknecht, A.; Fredrickson, G. H. *Macromolecules* **1999**, *32*, 6831.
(8) Zhao, M.; Sun, L.; Crooks, R. M. *J. Am. Chem. Soc.* **1998**, *120*, 4877.
(9) de Gennes, P.-G.; Hervet, H. *J. Phys. (Paris)* **1983**, *44*, L351.
(10) Lescanec, R. L.; Muthukumar, M. *Macromolecules* **1990**, *23*, 2280.
(11) Mansfield, M. L.; Klushin, L. I. *Macromolecules* **1993**, *26*, 4262.
(12) Boris, D.; Rubinstein, M. *Macromolecules* **1996**, *29*, 7251.
(13) Topp, A.; Bauer, B. J.; Klimash, J. W.; Spindler, R.; Tomalia, D. A.; Amis, E. J. *Macromolecules* **1999**, *32*, 7226.
(14) Lyulin, A. V.; Davies, G. R.; Adolf, D. B. *Macromolecules* **2000**, *33*, 6899.
(15) Welch, P.; Muthukumar, M. *Macromolecules* **2000**, *33*, 6159.
(16) Lue, L.; Prausnitz, J. M. *Macromolecules* **1997**, *30*, 6650.
(17) Milner, S. T. *Science* **1991**, *251*, 905.
(18) Milner, S. T.; Witten, T. A.; Cates, M. E. *Macromolecules* **1988**, *21*, 2610.
(19) Fleer, G.; Cohen-Stuart, M. A.; Scheutjens, J. M. H. M.; Cosgrove, T. Vincent, B. *Polymers at Interfaces*; Chapman and Hall: London, 1993.
(20) Pickett, G. T.; Balazs, A. C. *Macromol. Symp.* **1997**, *121*, 269.
(21) Singh, C.; Zhulina, E.; Gersappe, D.; Pickett, G. T.; Balazs, A. C. *Macromolecules* **1996**, *29*, 7637.
(22) Matsen, M. W.; Schick, M. *Phys. Rev. Lett.* **1994**, *72*, 2660.
(23) Pickett, G. T.; Witten, T. A. *Macromolecules* **1992**, *25*, 4569.
(24) Birshtein, T. M.; Mercurieva, A. A.; Klushin, L. I.; Polotsky, A. A.; *Comput. Theor. Polym. Sci.* **1998**, *8*, 179.
(25) Irvine, D. J,; Mayes, A. M.; Griffith-Cima, L. *Macromolecules* **1996**, *29*, 6037.
(26) Cui, S.-M.; Chen, Z. Y. *Phys. Rev. E* **1997**, *55*, 1660.
(27) Wormlike micelles, if they could be systematically end-grafted, could be a system where an annealed architecture would be involved.
(28) Press, W. H.; Teukolsky, S. A.; Vetterling, W. T.; Flannery, B. P. *Numerical Recipes in C;* Cambridge, 1992.
(29) In ref 12 the statistical weight to insert a monomer satisfies $g(z) = (1 - w\phi(z))$, whereas the correct statement is that $g(z) = \exp[-P(z)]$, where $P(z) = w\phi(z)$ ensures self-consistency. Thus, the calculations in ref 12 are quantitatively acceptable only for small $\phi(z)$.
(30) Carignano, M. A.; Szleifer, I. *Macromolecules* **1994**, *27*, 702.

MA010917Y